Reduction of optical chaos by a quantum correction in second-harmonic generation of light

K. Grygiel and P. Szlachetka
Nonlinear Optics Division, Institute of Physics, Adam Mickiewicz University, ul. Grunwaldzka 6, 60-780 Poznań, Poland
(Received 15 June 1994)

We consider the dynamics of second-harmonic generation of light in the context of chaos and order. The system is driven and dissipative. A Lyapunov analysis of chaos, and bifurcation maps, are presented and studied *versus* quantum corrections. We observe a reduction of chaos in the quantum case as well as suppression of basins of attraction. The role of damping is determined.

PACS number(s): 05.45.+b, 42.50.Lc

I. INTRODUCTION

In recent years, there has been a great deal of interest in the study of classically chaotic quantum systems. It is predominantly conceded that quantization drastically modifies classically chaotic behavior. For example, suppression of chaos to quasiperiodicity is observed in the quantum kicked rotator, whose classical counterpart behaves chaotically [1–2]. Certain manifestations of chaos become apparent in quantum dynamics [3–5] and quantum optics [6–9]. It seems that Wigner's formation of quantum mechanics offers the simplest comparison between quantum and classical chaos in contradistinction to the conventional procedure. The conventional way is to study how a wave packet initially fixed around a certain position q and momentum p follows the appropriate classical trajectory. However, this involves a disadvantage. Namely, the wave packet spreads in the course of time and is no longer sharply fixed around a particular position and momentum, rendering dubious the comparison with the respective classical trajectory. To avoid this spreading problem we can make use of the so-called Wigner symbols, their being a quantum generalization of classical variables. For example, we can compare the time evolution of the Wigner symbols for the position $\hat{q}$ and momentum $\hat{p}$ operators with the classical evolution of the position q and momentum p, respectively. Generally, Wigner's formulation of quantum mechanics leads to a c-number representation of the density matrix, that is, to the quantum analog of a classical probability density in (p,q) space. In quantum optics three kinds of c-number functions are the most popular, namely, the P representation, the Q function, and the Wigner function W [10]. All these three functions are defined in $(\alpha=p+iq,\ \alpha^*=p-iq)$ space instead of in (p,q) space. This is due to the coherent state technique. The P representation is related to normal ordering of the creation $\hat{a}^\dagger$ and annihilation $\hat{a}$ operators, the Q function is related to antinormal ordering of the operators, and the Wigner function W is related to symmetric (Weyl) ordering. The c-number approach makes it possible to treat quantum systems in a "classical way," including all their quantum features and contrasting the quantum and classical dynamics within the framework of a phase picture. The equations for the Wigner-like functions P and Q belong to the class of generalized Fokker-Planck equations whose solutions are known only for some simple optical models. The Wigner approach can also be used to study both kicked dynamics (that is, a quantum map) and a continuous flow. Kicked models are easier to analyze numerically than continuous models but are more difficult to verify practically. On the other hand, continuous models seem to be mathematically more cumbersome, resembling the complexity of hydrodynamical systems. In the latter case we usually make some truncations leading to a set of ordinary differential equations. Historically, for the first time in the treatment of classical dynamical systems, a truncation method has been used by Lorenz [11]. A similar truncation method can be used for generalized Fokker-Planck equations if we note that these equations generate a hierarchic and infinite set of ordinary differential equations for statistical cumulants. The first truncation always leads to equations having the form of classical equations of motion. The second truncation plays the role of the first quantum correction, etc. Recently, the cumulant method has been applied to the study of some aspects of classical and quantum chaos in second-harmonic generation of light [12–15] and an oscillator with Kerr nonlinearity [16]. To identify chaotic behavior of a classical dynamical system it suffices to use the maximal Lyapunov exponent (MLE). A quantum analog of the Lyapunov exponent involving the Q function has been proposed by Toda and Ikeda [17]. However, as we have already mentioned, the equation for the Q (P,W) function is mathematically cumbersome and its analytic solution is unknown for most nonlinear systems. This poses additional difficulties when it comes to calculating the Lyapunov exponents. However, this problem can be solved indirectly and approximately by finite cumulant expansion [16], enabling us to use the classical calculation method of MLE for equations with statistical cumulants.

In this paper we consider the dynamics of a truncated model of second-harmonic generation. Ours is based on a Fokker-Planck equation for the quasidistribution function $P(Q)$. The model proposed and the truncation procedure are briefly reviewed in Secs. II and III. In Sec. IV we investigate the qualitative behavior of the model in dependence on its characteristic parameters: the form of the external driving field and the damping constants.

The stability of our system (the appearance and disappearance of the chaotic region) is studied with the help of Lyapunov analysis. We observe a reduction of chaos in the system, classically chaotic previous to quantum correction. The whole dynamics is also presented in the form of bifurcation maps and, for certain parameters, in that of phase portraits in both classical and quantum cases.

II. MODEL

Let us consider an optical system with two interacting modes at the frequencies ω_1 and $\omega_2=2\omega_1$, respectively, interacting by way of a nonlinear crystal with second-order susceptibility. Moreover, let us assume that the nonlinear crystal is placed within a Fabry-Pérot interferometer. Both modes are damped via a reservoir. The fundamental mode is driven by an external field with the frequency ω_L and amplitude F. The Hamiltonian for our system is given by [18,19]

$$\hat{H}=\hat{H}_{\rm rev}+\hat{H}_{\rm irrev} , \tag{1}$$

$$\hat{H}_{\rm rev}=\hbar\omega_1\hat{a}_1^{\dagger}\hat{a}_1+\hbar\omega_2\hat{a}_2^{\dagger}\hat{a}_2+i\hbar F(\hat{a}_1^{\dagger}e^{-i\omega_L t}-\hat{a}_1 e^{i\omega_L t}) +i\hbar\frac{\chi}{2}(\hat{a}_1^{\dagger 2}\hat{a}_2-\hat{a}_1^2\hat{a}_2^{\dagger}) , \tag{2}$$

$$\hat{H}_{\rm irrev}=\hbar\sum_j\sum_{i=1}^{2}(\Omega_j^{(i)}\hat{b}_j^{\dagger(i)}\hat{b}_j^{(i)}+K_j^{(i)}\hat{b}_j^{(i)}\hat{a}_i^{\dagger} +K_j^{*(i)}\hat{b}_j^{\dagger(i)}\hat{a}_i) , \tag{3}$$

where $\hat{H}_{\rm rev}$ describes the reversible part of interaction, and $\hat{H}_{\rm irrev}$ is the irreversible part responsible for the loss mechanism. The quantities $\hat{a}_1(\hat{a}_1^{\dagger})$; $\hat{a}_2$ $(\hat{a}_2^{\dagger})$ are the photon annihilation (creation) operators for the fundamental and second-harmonic modes, respectively. The parameter χ is taken to be real and acts as the nonlinear coupling constant between the two modes. Finally, the operators $\hat{b}_j^{\dagger(i)}$, $\hat{b}_j^{(i)}$ are the boson annihilation (creation) operators of the reservoir. The frequencies of the reservoir oscillations are denoted by $\Omega_j^{(i)}$ and the coupling constant between the optical and reservoir modes by $K_j^{(i)}$. The dynamics of the system (1) on eliminating the reservoir Hamiltonian (3) is governed by the appropriate master equation for the density operator ρ. The master equation in the interaction picture leads to the following c-number Fokker-Planck equation for the quasidistribution function $\Phi_{(s)}$ [10,18,19],

$$\frac{\partial\Phi_{(s)}}{\partial\tau}=L_{\rm irrev}+L_{\rm rev} , \tag{4}$$

where

$$L_{\rm irrev}=\sum_{i=1}^{2}\left[\Gamma_i\frac{\partial}{\partial\alpha_i}(\alpha_i\Phi_{(s)})+\Gamma_i\frac{\partial}{\partial\alpha_i^*}(\alpha_i^*\Phi_{(s)}) +\Gamma_i\left[n_i+\frac{1-s}{2}\right]\frac{\partial^2\Phi_{(s)}}{\partial\alpha_i^*\partial\alpha_i}\right] , \tag{5}$$

$$L_{\rm rev}=\sum_{i=1}^{2}\left[\frac{\partial}{\partial\alpha_i}(D_i\Phi_{(s)})+\frac{\partial}{\partial\alpha_i^*}(D_i^*\Phi_{(s)})\right] -\frac{s}{2}\frac{\partial^2}{\partial\alpha_1^2}(D_{11}\Phi_{(s)})-\frac{s}{2}\frac{\partial^2}{\partial\alpha_1^{*2}}(D_{11}^*\Phi_{(s)}) . \tag{6}$$

The quasidistribution function $\Phi_{(s)}$ is defined as follows: $\Phi_{(s=1)}=P$ and $\Phi_{(s=-1)}=Q$. The function $\Phi_{(s)}$ is determined in the complex plane $(\alpha_1,\alpha_2,\alpha_1^*,\alpha_2^*)$, where α_i is an eigenvalue of the annihilation operator $\hat{a}_i$, i.e., $\hat{a}_i|\alpha_i\rangle=\alpha_i|\alpha_i\rangle$. Here, $|\alpha_i\rangle$ is a coherent state. The initial condition for the Fokker-Planck equation is given by

$$\Phi_{(s)}[\alpha_1(\tau),\alpha_2(\tau);\tau]|_{\tau=0}=\Phi_{(s)}[\alpha_1(0)=\alpha_{10},\alpha_2(0)=0;0] , \tag{7}$$

which means that, at the start, the amplitude of the fundamental mode differs from zero, whereas the amplitude of the second harmonic equals zero. The coefficients D_i and D_{11} are given by [20]

$$\begin{aligned} D_1&=-\mathcal{F}-\alpha_1^*\alpha_2 , \\ D_1^*&=-\mathcal{F}-\alpha_1\alpha_2^* , \\ D_2&=0.5\alpha_1^2 , \\ D_2^*&=0.5\alpha_1^{*2} , \\ D_{11}&=\frac{\partial D_1}{\partial\alpha_1^*}=-\alpha_2 , \\ D_{11}^*&=\frac{\partial D_1^*}{\partial\alpha_1}=-\alpha_2^* . \end{aligned} \tag{8}$$

The quantities Γ_1 and Γ_2 are the damping constants for the fundamental and second-harmonic modes, respectively. In Eq. (6) we shall restrict ourselves to the case of zero frequency mismatch between the cavity and the external forces $(\omega_1-\omega_L=0)$. In this way we exclude the rapidly oscillating terms. Moreover, the time t and the external amplitude F have been redefined as follows:

$$\tau=\chi t , \quad \mathcal{F}=\frac{F}{\chi} . \tag{9}$$

The s ordering in Eq. (4), which is responsible for the operator structure of the Hamiltonian, allows us to contrast the classical and quantum dynamics of our system. If the Hamiltonian [(1)–(3)] is classical (i.e., if it is a c number), then the equation for the probability density has the form of Eq. (4) without the s terms: $-(s/2)(\partial^2/\partial\alpha_1^2)(D_{11}\Phi_{(s)})-(s/2)(\partial^2/\partial\alpha_1^{*2})(D_{11}^*\Phi_{(s)})$ and $\Gamma_i((1-s)/2)\partial^2\Phi_{(s)}/\partial\alpha_i^*\partial\alpha_i$. The s terms distinguish the classical and quantum dynamics quite naturally. If they do not appear, the difference between P and Q vanishes. The same interpretation of $\Phi_{(s)}$ for the anharmonic oscillator model is presented in [16].

III. TRUNCATION

Analytic solutions of quantum Fokker-Planck equations like Eq. (4) are known only in special cases. Thus,

some special methods have been developed to obtain approximate solutions. One of them is the statistical moment method, based on the fact that the equation for the probability density generates an infinite hierarchic set of equations for the statistical moments and *vice versa*. However, for numerical reasons, the set of equations has to be truncated to a finite number, which means approximation. Below, we use cumulants as statistical moments and restrict ourselves to a Gaussian approximation (cumulants higher than second order are equal to zero) [12,16].

The cumulants are defined by the following relations:

$$\xi_i=\langle \hat{a}_i \rangle \ , \tag{10}$$

$$B_i=\langle \hat{a}_i^\dagger \hat{a}_i \rangle-\langle \hat{a}_i^\dagger \rangle\langle \hat{a}_i \rangle \ , \tag{11}$$

$$B_{12}=\langle \hat{a}_1^\dagger \hat{a}_2 \rangle-\langle \hat{a}_1^\dagger \rangle\langle \hat{a}_2 \rangle \ , \tag{12}$$

$$C_i=\langle \hat{a}_i^2 \rangle-\langle \hat{a}_i \rangle^2 \ , \tag{13}$$

$$C_{12}=\langle \hat{a}_1 \hat{a}_2 \rangle-\langle \hat{a}_1 \rangle\langle \hat{a}_2 \rangle \ . \tag{14}$$

Integration by parts of the Fokker-Planck equation for the quasidistribution $\Phi_{(s=1)}=P$ (the choice of a particular s is a question of taste only) allows us to write the appropriate equations for the cumulants [10,16,19,21]. In what follows, we assume that damping is included only by way of coupling to the reservoir at zero temperature, that is, $n_i=0$. The first truncation (the cumulants higher than first-order vanish) leads to the classical limit. Then, from Eq. (4), we get the classical Bloembergen equations [12]:

$$\frac{d\xi_1}{d\tau}=-\Gamma_1\xi_1+\mathcal{F}+\xi_1^*\xi_2 \ , \tag{15}$$

$$\frac{d\xi_2}{d\tau}=-\Gamma_2\xi_2-0.5\xi_1^2 \ . \tag{16}$$

The initial conditions have the form

$$\xi_1(0)=\xi_{10} \ , \quad \xi_2(0)=0 \ . \tag{17}$$

The s terms in Eq. (4) contribute nothing to the above equations. The second-order truncation (Gaussian approximation) leads to the following set of equations:

$$\frac{d\xi_1}{d\tau}=-\Gamma_1\xi_1+\mathcal{F}+\xi_1^*\xi_2+B_{12} \ , \tag{18}$$

$$\frac{d\xi_2}{d\tau}=-\Gamma_2\xi_2-0.5(\xi_1^2+C_1) \ , \tag{19}$$

$$\frac{dB_1}{d\tau}=-2\Gamma_1B_1+B_{12}^*\xi_1+B_{12}\xi_1^*+C_1^*\xi_2+C_1\xi_2^* \ , \tag{20}$$

$$\frac{dB_2}{d\tau}=-2\Gamma_2B_2-B_{12}^*\xi_1-B_{12}\xi_1^* \ , \tag{21}$$

$$\frac{dC_1}{d\tau}=-2\Gamma_1C_1+2(C_{12}\xi_1^*+B_1\xi_2)+\xi_2 \ , \tag{22}$$

$$\frac{dC_2}{d\tau}=-2\Gamma_2C_2-2C_{12}\xi_1 \ , \tag{23}$$

$$\frac{dC_{12}}{d\tau}=-(\Gamma_1+\Gamma_2)C_{12}+B_{12}\xi_2-C_1\xi_1+C_2\xi_1^* \ , \tag{24}$$

$$\frac{dB_{12}}{d\tau}=-(\Gamma_1+\Gamma_2)B_{12}+C_{12}\xi_2^*+\xi_1(B_2-B_1) \ . \tag{25}$$

The set of Eqs. (18)–(25), proposed for the first time by Peřina *et al.* [19], is a development of the Bloembergen equations [(15) and (16)]. The initial conditions with respect to (7) are given by

$$\begin{aligned}&\xi_1(0)=\xi_{10} \ , \quad \xi_2(0)=0 \ ,\\ &B_{1,2}(0)=B_{12}(0)=C_{1,2}(0)=C_{12}(0)=0 \ .\end{aligned} \tag{26}$$

The s terms in Eq. (4) contribute only the term ξ_2 in Eq. (22). Thus, the term ξ_2 represents the quantum diffusional s terms in the Fokker-Planck equation. The other terms in Eqs. (18)–(25) originate in the drift terms of the Fokker-Planck equation. The terms B_{12} and C_1 in Eqs. (18) and (19) play the role of feedback terms that pump quantum fluctuations into the classical Bloembergen equations. If the s terms in Eq. (4) do not appear (the classical case) the term ξ_2 in Eq. (22) does not appear either. In this case the subset [(20)–(25)] with zero initial conditions has zero solutions and consequently leads to the first truncation [12]. The aspects of higher-order truncation for nonlinear optical problems are discussed in [12,16].

IV. NUMERICAL ANALYSIS

To identify chaotic behavior of a classical dynamical system, it is convenient to use the maximal Lyapunov exponent [22]. The MLE characterizes the degree of orbital instability, i.e., the rate of divergence of the distance between two nearby orbits. In order to get the MLE, we use the following procedure. On applying variations $\xi_i\rightarrow\xi_i+\delta_i$ and with regard to (15) and (16), we get the following linearized equations for the complex increment δ_i:

$$\frac{d\delta_1}{d\tau}=-\Gamma_1\delta_1+\delta_1^*\xi_2+\xi_1^*\delta_2 \ , \tag{27}$$

$$\frac{d\delta_2}{d\tau}=-\Gamma_2\delta_2-\delta_1\xi_1 \ . \tag{28}$$

Now, having the two sets of equations [(15) and (16) and (27) and (28)] available, we can compute

$$\lambda=\lim_{\tau\rightarrow\infty}\lambda_\tau \ , \tag{29}$$

where

$$\lambda_\tau=\frac{1}{\tau}\ln\left[\sum_{i-1}^{2}\{[\mathrm{Re}\delta_i(\tau)]^2+[\mathrm{Im}\delta_i(\tau)]^2\}\right]^{1/2} \ . \tag{30}$$

The quantity λ is referred to as the MLE. The positive MLE points to chaotic motion. If $\lambda\leq 0$, the dynamical system behaves nonchaotically (orderly). The definition of quantum Lyapunov exponents has been considered by several authors [17,23].

The concept of the classical MLE can be applied with some modification to the quantum equations (18)–(25). The modification originates in the fact that the concept of trajectory loses its meaning in quantal dynamics so the

classical Lyapunov exponents cannot be directly used in quantum systems. Moreover, classical chaos is accommodated in a quantum dynamics as a transient process with a finite lifetime $\tau=\tau_{\text{quant}}$. It is known that for the time $\tau>\tau_{\text{quant}}$ the behavior of quantum systems is quasiperiodic. Thus, the quantum Lyapunov exponent whose classical counterpart is positive has to be calculated as (29), but with a finite time (empirically expressed) $\tau=\tau_{\text{quant}}$, where $\tau_{\text{quant}}=\ln(A_R/\hbar)/\lambda$. The quantity A_R is the space area available for the classical motion, and the quantity λ is the classical Lyapunov exponent. The time τ_{quant} has been introduced by Berman and Kolovsky [24].

Let us note that in the quantum case, we deal with 14 equations of motion in real variables [B_1 and B_2 in (18)–(25) are real]. By adding 14 linearized equations of motion for the increments δ_i, we obtain 28 equations of motion, which can be solved numerically. Below, we discuss the behavior of our system if the external driving field $\mathcal{F}(\tau)$ is periodically modulated.

A. External driving field $\mathcal{F}=\mathcal{F}_0(1+\sin\Omega\tau)$

Let us consider the driving field amplitude in the form $\mathcal{F}=\mathcal{F}_0(1+\sin\Omega\tau)$, meaning that the external pump amplitude is modulated with a frequency Ω around $\mathcal{F}_0$ [13]. For the time-independent field $\mathcal{F}=\mathcal{F}_0$ ($\Omega=0$) the system does not manifest chaotic behavior. However, a change of Ω in the range $0<\Omega<7$ leads the system from periodic to chaotic motion or *vice versa*. The dynamical behavior of our system is reflected by the Lyapunov exponents. The MLE as a function of the modulation parameter Ω for the classical case [Eqs. (15) and (16)] (dashed line) and for the quantum case [Eqs. (18)–(25)] (solid line) is plotted in Fig. 1(a). For the classical case, one observes several regions where the system behaves chaotically ($\lambda>0$), whereas elsewhere it behaves orderly ($\lambda<0$). For the quantum case, we observe only one region of chaos $1.3<\Omega<1.72$, which does not overlap exactly any classical region of chaos. Generally, as is seen from Fig. 1(a), the quantum correction reduces chaos in the system but does not eliminate it completely. For example, for $\Omega=1.4$, both the classical and quantum versions of the system behave chaotically, whereas the classical MLE is greater than quantum. This means a reduction of chaos in the classical system due to the quantum correction. The reduction is also reflected by the appropriate bifurcation diagrams [Figs. 1(b) and 1(c)]. Another useful way to visualize the reduction of chaos is to analyze the motion in the phase space. However, in our case, the classical phase space is four dimensional (Re ξ_1, Re ξ_2, Im ξ_1, Im ξ_2). This means that we can compare only the motion in the reduced phase space. For a physical interpretation it is convenient to consider the motion in two-dimensional intensity space $I_1=|\xi_1|^2$, $I_2=|\xi_2|^2$. Then, instead of a typical *phase portrait* we deal with *an intensity portrait*. In the quantum case the intensities are the average numbers of photons determined by $\langle\hat{a}_i^{\dagger}\hat{a}_i\rangle=|\xi_i|^2+B_i$, where B_i is the quantum correction to the classical intensity $I_i=|\xi_i|^2$.

The reduction of chaos for $\Omega=1.45$ is presented in the intensity portraits of Fig. 2. However, as is seen from Fig. 1(a), there is a small region ($1.68<\Omega<1.80$) where the system behaves orderly in the classical case but the quantum correction leads to chaos. By way of an example for $\Omega=1.75$, the classical system, after quantum correction, loses it orderly features and the limit cycle [Fig. 3(a)] settles into a chaotic trajectory [Fig. 3(b)]. Generally, Lyapunov analysis shows that the transition from classical chaos to quantum order is very common. For example, this kind of transition appears for $\Omega=3.5$

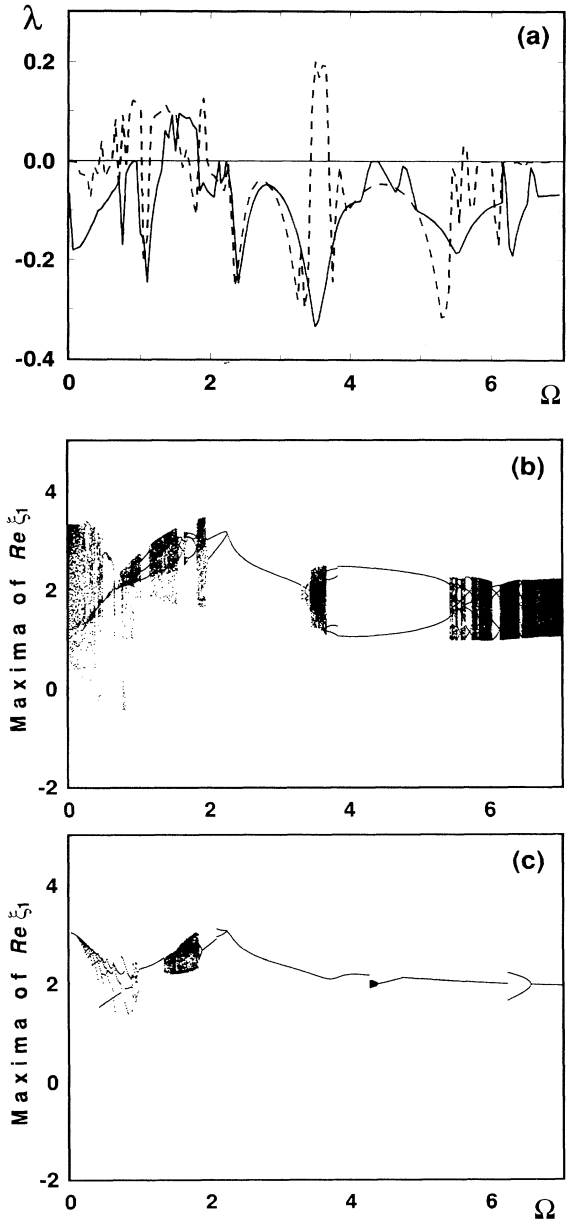

FIG. 1. The classical (dashed) and quantum (solid line) MLE's (a) and the appropriate bifurcation maps [(b) and (c)] versus the modulated parameter Ω. The parameters are $\xi_1(0)=0.1+i0.1$, $\xi_2(0)=0$, $B_{1,2}(0)=B_{12}(0)=C_{1,2}(0)=C_{12}(0)=0$, $\Gamma_1=\Gamma_2=0.34$, and $\mathcal{F}_0=2$.

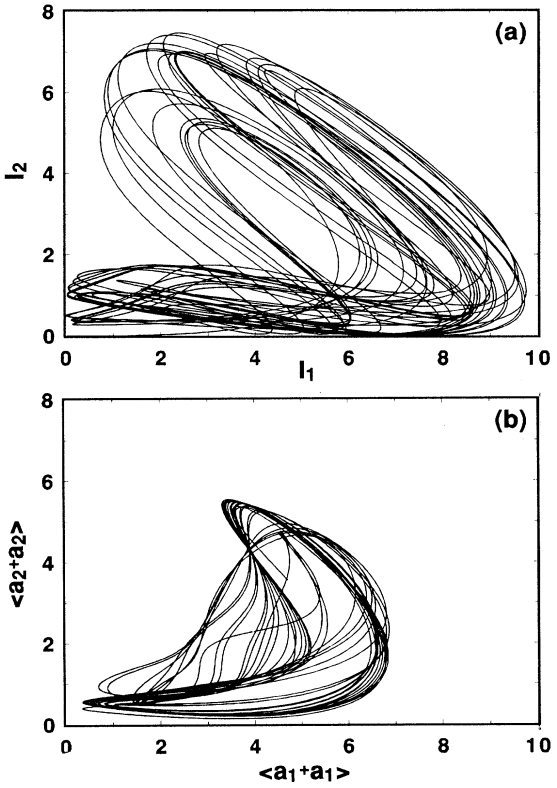

FIG. 2. Transition from classical chaos (a) to quantum chaos (b). The parameters are those of Fig. 1, but with $\Omega = 1.4$.

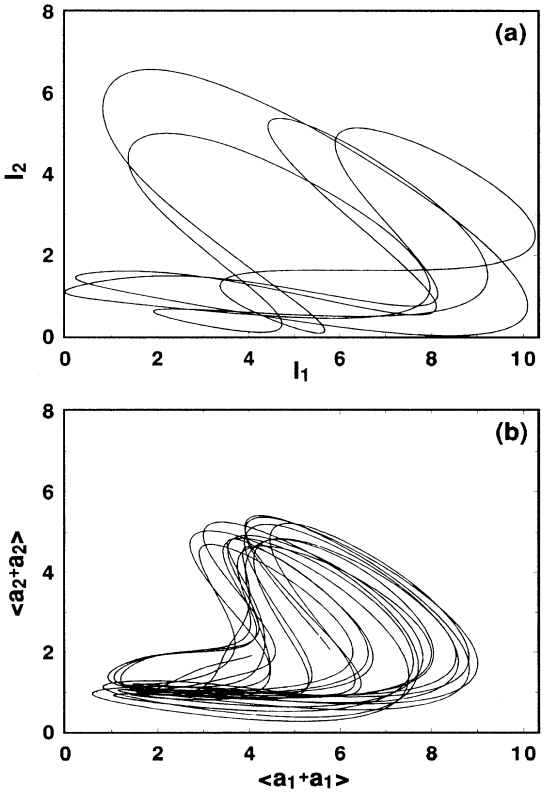

FIG. 3. Transition from classical order (a) to quantum chaos (b). The parameters are those of Fig. 1, but with $\Omega = 1.75$.

where chaos is reduced to periodic motion on a limit cycle. Therefore, a global reduction of chaos can be said to take place in the whole region of the parameter $0 < \Omega < 7$. As we see from Fig. 1, there are also possible transitions leading from classical order to quantum order. For example, for $\Omega = 6.7$, the quasiperiodic classical motion on a torus is reduced to periodic motion on a limit circle after the quantum correction.

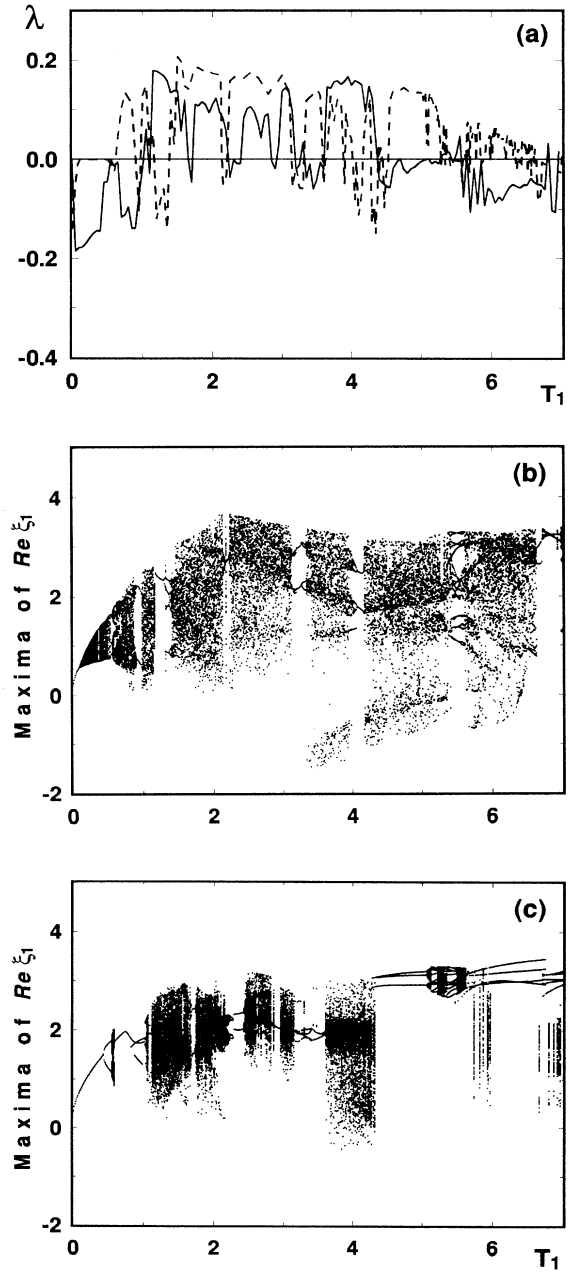

FIG. 4. The classical (dashed) and quantum (solid line) MLE's (a) and the appropriate bifurcation maps [(b) and (c)] versus the pulse length T_1. The parameters are $\xi_1(0) = 0.1 + i0.1$, $\xi_2(0) = 0$, $B_{1,2}(0) = B_{12}(0) = C_{1,2}(0) = C_{12}(0) = 0$, $\Gamma_1 = 0$, $\Gamma_2 = 0.34$, and $\mathcal{F}_0 = 2$.

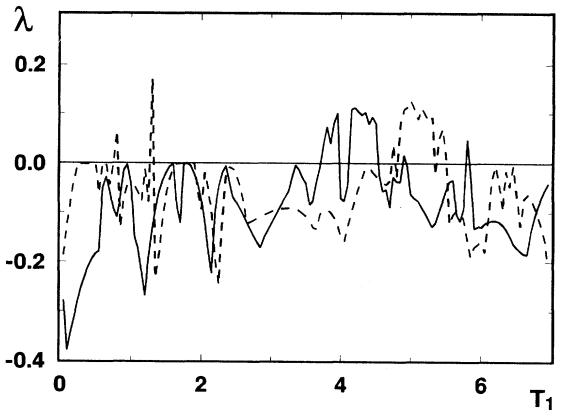

FIG. 5. The classical (dashed) and quantum (solid line) MLE's versus the pulse length T_1. The parameters are $\xi_1(0)=0.1+i0.1$, $\xi_2(0)=0$, $B_{1,2}(0)=B_{12}(0)=C_{1,2}(0)=C_{12}(0)=0$, $\Gamma_1=0.17$, $\Gamma_2=0.34$, and $\mathcal{F}_0=2$.

B. External driving field as a train of rectangular pulses

An analysis of the classical system described by Eqs. (15) and (16) with external driving field in the form of a train of pulses has been proposed by us in [14,15]. The external driving field in the form of a train of pulses is simulated by computer. The pulse length is denoted by T_1 and the height of the pulse by $\mathcal{F}_0$. The distance between two pulses is denoted by T_2. It is interesting to investigate the influence of quantum correction on the dynamics of the classical system [(15) and (16)]. In this section, we consider the problem restricting ourselves only to the study of MLE's and bifurcation diagrams for different damping constants Γ_1. Generally, we can observe similar transitions from chaos to order and order to chaos as in the case of externally modulated amplitude $\mathcal{F}=\mathcal{F}_0(1+\sin\Omega\tau)$. What is the role of the damping constants in the reduction of chaos? In Fig. 4 we present the MLE as a function of the pulse length T_1 for both the classical (dashed line) and quantum (solid line) case and the respective bifurcation maps for the damping constants $\Gamma_1=0$, $\Gamma_2=0.34$. Figures 5 and 6 present the respective Lyapunov exponent for different damping constants, namely, $\Gamma_1=0.17$, $\Gamma_2=0.34$, and $\Gamma_1=\Gamma_2=0.34$. Figures 4, 5, and 6 show that the reduction of chaotic regions ($\lambda>0$) takes place with growing damping constant Γ_1. It is caused by the fact that the stability of the system generally depends on damping. It is seen from the Lyapunov spectra and bifurcation maps that the quantum system is similarly sensitive to damping as the classical system. However, quantum chaos is more strongly suppressed than classical chaos.

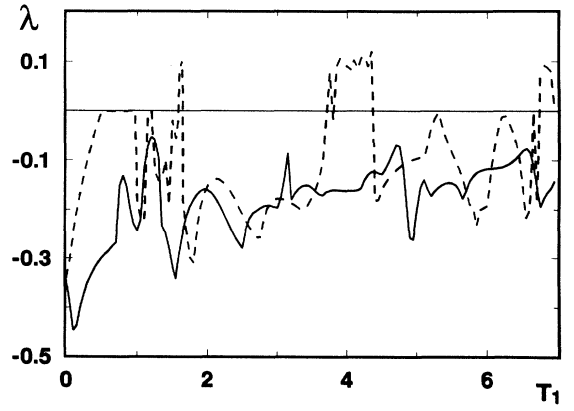

FIG. 6. The same as in Fig. 5, but with $\Gamma_1=0.34$.

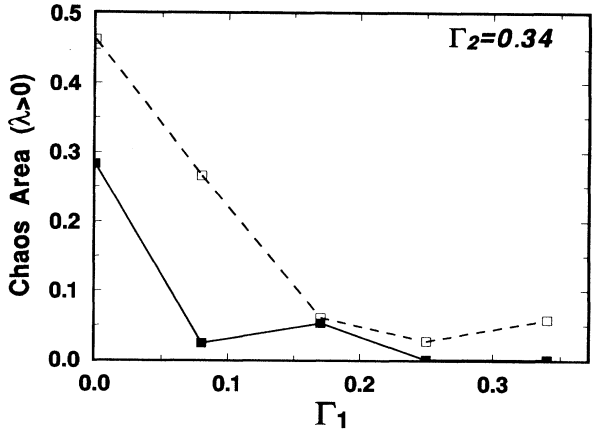

FIG. 7. Chaos area as a function of the damping constant Γ_1. The classical case, dashed line; the quantum case, solid line.

V. CONCLUSION

Our paper considers mainly the influence of quantum correction on the behavior of a system (second-harmonic generation) that is classically chaotic. The system is damped and pumped by an external driving field. Its dynamics are governed by a set of ordinary differential equations resulting from the Fokker-Planck equation. The appearance and size of the chaotic and orderly regions depend on the form of the external driving field. The regions of chaos for the classical model do not overlap exactly the chaotic regions for the quantum model. However, we find that quantum correction reduces chaos in the classical system. The Lyapunov analysis and bifurcation maps show that after the quantum correction, the number of chaotic regions is reduced, although not eliminated completely. Nonetheless we observe some similarities between the quantum and classical bifurcation maps. Namely, within certain regions of the parameter Ω both bifurcation maps differ slightly and this can be observed in Figs. 1(b) and 1(c). The changes in the dynamics are also manifested in the intensity portraits. For example, Figs. 2 and 3 show that the basin of attraction is always suppressed after quantum correction. In Fig. 7, we plot the area of chaos as a function of the damping constant Γ_1. By way of example, the value 0.46 for $\Gamma_1=0$ is the value of the integrated field in Fig. 4(a) under the dashed line, satisfying the condition $\lambda>0$. This value is a measure of classical chaos in the global sense for the region $0<T_1<7$. From Fig. 7, it is clear that the quantum chaotic system is always more strongly suppressed than its classical counterpart.

[1] G. Casati, B. Chirkov, J. Ford, and F. M. Izrailev, in *Stochastic Behavior in Classical and Quantum Hamiltonian Systems,* edited by G. Casati and J. Ford, Lecture Notes in Physics Vol. 93 (Springer, Berlin, 1979).
[2] D. L. Shepelyansky, Physics D **28**, 103 (1987).
[3] P. W. Milonni, M. L. Shih, and J. R. Ackerhalt, *Chaos in Laser-matter Interactions* (World Scientific, Singapore, 1987).
[4] Y. Pomeau, B. Dorizzi, and B. Grammaticos, Phys. Rev. Lett. **56**, 681 (1986).
[5] P. W. Milonni, J. R. Ackerhalt, and M. E. Goggin, Phys. Rev. A **35**, 1714 (1987).
[6] C. C. Gerry and E. R. Vrscay, Phys. Rev. A **39**, 5717 (1989).
[7] G. J. Milburn, Phys. Rev. A **41**, 6567 (1990).
[8] G. J. Milburn and C. A. Holms Phys. Rev. A **44**, 4704 (1991).
[9] *Instabilities and Chaos in Quantum Optics,* edited by F. T. Arecchi and R. H. Harrison (Springer-Verlag, Berlin, 1987).
[10] J. Peřina, *Quantum Statistics of Linear and Nonlinear Optical Phenomena,* 2nd ed. (Reidel, Dordrecht, 1991).
[11] E. N. Lorenz, J. Atmos. Sci. **20**, 130 (1963).
[12] P. Szlachetka, K. Grygiel, J. Bajer, and J. Peřina, Phys. Rev. A **46**, 7311 (1992).
[13] K. Grygiel and P. Szlachetka, Opt. Commun. **78**, 177 (1990).
[14] K. Grygiel and P. Szlachetka, Opt. Commun. **91**, 241 (1992).
[15] P. Szlachetka and K. Grygiel, in *Symmetry and Structural Properties of Condensed Matter,* Proceedings of the Second International School of Theoretical Physics, Poznań 1992, edited by W. Florek, D. Lipiński, and T. Lulek (World Scientific, Singapore, 1993), pp. 221–236.
[16] P. Szlachetka, K. Grygiel, and J. Bajer, Phys. Rev. E **48**, 101 (1993).
[17] M. Toda and K. Ikeda, Phys. Lett. A **124**, 165 (1987).
[18] P. D. Drummond, K. J. McNeil, and D. F. Walls, Opt. Acta **27**, 321 (1980); **28**, 211 (1981).
[19] J. Peřina *et al.* Czech. J. Phys. B **37**, 1161 (1987).
[20] The general relations among the coefficients D_i, $D_{ij}, \ldots, D_{ijk\cdots m}$ for the irreversible part of Fokker-Planck equations are presented in P. Szlachetka, J. Phys. A **20**, 1455 (1987).
[21] R. Schack and A. Schenzle, Phys. Rev. A **41**, 3847 (1990).
[22] J. P. Eckmann and D. Ruelle, Rev. Mod. Phys. **57**, 617 (1985).
[23] F. Hakke, H. Wiedemann, and K. Życzkowski, Ann. Phys. **1**, 531 (1992).
[24] G. P. Berman and A. R. Kolovsky, Physica D **8**, 117 (1983).